Investigating Laser-Induced Phase Engineering in MoS₂ Transistors

Papadopoulos, Nikos; Island, Joshua O.; van der Zant, Herre S.J.; Steele, Gary A.

DOI
10.1109/TED.2018.2855215

Publication date
2018

Published in
IEEE Transactions on Electron Devices

Investigating Laser-Induced Phase Engineering in MoS_2 Transistors

Nikos Papadopoulos, Joshua O. Island, Herre S. J. van der Zant, and Gary A. Steele

***Abstract*— Phase engineering of MoS_2 transistors has recently been demonstrated and has led to record low contact resistances. The phase patterning of MoS_2 flakes with laser radiation has also been realized via spectroscopic methods, which invites the potential of controlling the metallic and semiconducting phases of MoS_2 transistors by simple light exposure. Nevertheless, the fabrication and demonstration of laser-patterned MoS_2 devices starting from the metallic polymorph have not been demonstrated yet. Here, we study the effects of laser radiation on 1T/1T′-MoS_2 transistors with the prospect of driving an *in situ* phase transition to the 2H-polymorph through light exposure. We find that although the Raman peaks of 2H-MoS_2 become more prominent and the ones from the 1T/1T′ phase fade after the laser exposure, the semiconducting properties of the laser-patterned devices are not fully restored, and the laser treatment ultimately leads to the degradation of the transport channel.**

***Index Terms*— Laser patterning (LP), molybdenum disulfide, phase transition, transistors.**

I. Introduction

THE transition metal dichalcogenides (TMDCs) form a large family of layered materials that have been studied extensively in the past few years [1]–[4]. 2H-MoS_2 is one of the most well known in this family with a direct optical bandgap of 1.8 eV [5], which becomes indirect and decreases as the number of the layers increases, reaching 1.3 eV in bulk [6]. These properties render 2H-MoS_2 ideal for applications such as field-effect transistors (FETs) [7], photodetectors [8], and light emitting diodes (LEDs) [9]. A striking difference between TMDCs and other 2-D materials like graphene is the polymorphism of these materials [2]. Naturally occurring semiconducting MoS_2 has a trigonal prismatic structure (2H-MoS_2). Another known polymorph is 1T-MoS_2 with an octahedral geometry [10], [11], which has metallic properties and stabilizes with lattice distortion by forming the so-called 1T′-MoS_2, where the clustering of Mo atoms takes place with the formation of various superstructures [12]. A known route to obtain the 1T/1T′ phase is via chemical doping usually by using *n*-butyl lithium (BuLi), where Li atoms donate an electron to the Mo atoms [13]. The dynamics and the mechanisms of intercalation and the phase transformation in MoS_2 have been studied by several groups in recent years [12], [14]–[17]. These studies have shown that the 1T and 1T′ phases coexist (1T/1T′ phase), and the 1T/1T′ phase is present even after removal of the lithium with more metallic properties than the natural polytype [13].

1T/1T′-MoS_2 is metastable with relaxation energy of ∼1 eV and relaxes to the 2H phase with annealing above 95 °C [11] or with extensive aging [18]. Another route to induce a metallic to semiconducting transition is via laser heating as shown recently by two different groups [19], [20]. This approach is intriguing as the phase transformation takes place locally and provides the opportunity to form in-plane heterostructures [21]. This type of heterostructure is interesting for TMDCs as 1T/1T′ contacted MoS_2 [22], [23] and WSe_2 [24] FETs show lower contact resistance and superior device characteristics [25]. Also, such heterostructures could be used for catalytic processes. Nevertheless, the fabrication of such planar heterostructures via laser patterning (LP) and their properties has not yet been explored.

Here, we investigate patterning of the semiconducting phase of MoS_2 via laser-induced local heating in a few-layer FET. We use a green laser light at 515 nm and monitor the transformation processes via Raman spectroscopy. Moreover, we extract the range of the laser power that should be used for such process by analyzing the Raman spectra. Thereafter, we investigate the laser-scribed planar MoS_2 heterostructures in various FET devices and the impact of the consecutive phase transitions on the characteristics of the devices.

II. Results and Discussion

The semiconducting to metallic transition in MoS_2 was achieved by chemical doping in *n*-butyllithium solution (1.6 M in hexane, Sigma Aldrich) inside a glove box environment. Usually, with this treatment, the samples can reach 50% of the 1T/1T′ phase within a flake [21], [26]. We used optical imaging, Raman, photoluminescence spectroscopy as well as electrical measurements for the characterization of the transition. In Fig. 1(a) and (b), the optical images of a thin MoS_2 flake (four to five layers) before and after the

Manuscript received April 6, 2018; revised June 8, 2018; accepted July 8, 2018. Date of publication July 27, 2018; date of current version September 20, 2018. This work is under a project of the Netherlands Organization for Scientific Research (NWO). The review of this paper was arranged by Editor S. Das. *(Corresponding author: Nikos Papadopoulos.)*

The authors are with the Kavli Institute of Nanoscience, Delft University of Technology, 2628 CJ Delft, The Netherlands (e-mail: n.papadopoulos@tudelft.nl).

Color versions of one or more of the figures in this paper are available online at http://ieeexplore.ieee.org.

Digital Object Identifier 10.1109/TED.2018.2855215

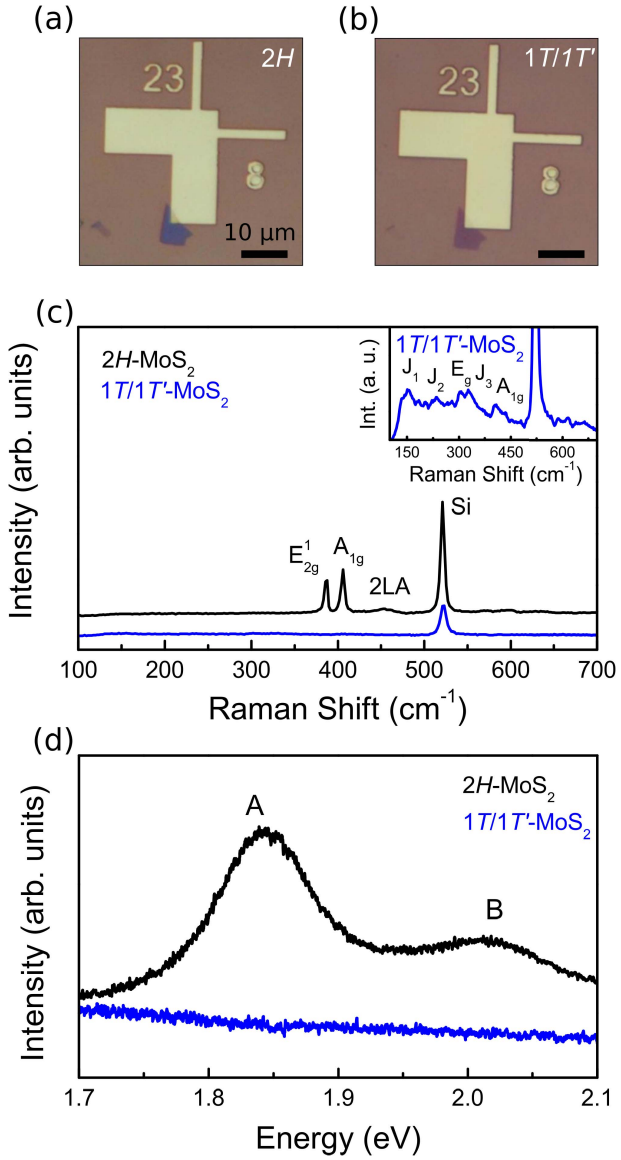

Fig. 1. Semiconducting to metallic transition in MoS_2 via chemical doping. Optical images of a few-layer MoS_2 (a) before and (b) after the treatment with *n*-butyl lithium, where the change in the color is attributed to the phase transition. (c) Raman spectra of the 2H and 1T/1T′ phases of MoS_2. Inset: spectra of the 1T/1T′-MoS_2 from with a different range on the *y*-axis. The J_1, J_2, and J_3 peaks from the 1T/1T′ phase are visible. (d) Photoluminescence spectra of the 2H and 1T/1T′ of MoS_2. The A and B excitonic peaks in the case of the 1T/1T′-MoS_2 are quenched.

immersion in BuLi show the change in the optical properties of the material. Unambiguously, the color and contrast of the flake after the bath have changed similar to other studies [27]. Raman spectroscopy is a powerful technique to study structural changes and chemical bonds in materials and molecules. Different crystal structures that arise after the chemical doping can be easily probed with Raman spectroscopy. In Fig. 1(c), the Raman spectra of 2H-MoS_2 and 1T/1T′-MoS_2 are depicted, which were obtained with low power (<0.05 mW/μm^2) to avoid any heating effects. In the case of the 1T/1T′-MoS_2, the absence of the in-plane E^1_{2g} peak and the weak A_{1g} peak at 404 cm^{-1} together with the presence of small features at 155, 233, and 331 cm^{-1} confirms the structural arrangement of the atoms in an octahedral and a distorted octahedral lattice [see inset of Fig. 1(c)]. The three weak peaks are the J_1, J_2, and J_3 modes, which arise from the formation of a $2a_0 \times a_0$ superlattice, probably as a result of a Peierls [28] or a Jahn–Teller instability [12] and the clustering of Mo atoms into chains [18], [29], [30]. Apart from the quenching of the Raman peaks of the 2H phase, the A and B exciton peaks of the photoluminescence spectra were also quenched [Fig. 1(d)], confirming the partial change to the 1T/1T′ polymorph.

For the transformation and the recovery of the semiconducting properties of the MoS_2 flakes and FETs, we used laser radiation at 515 nm with a 100× objective with a spot of ~0.5 μm^2. To find out the right power that can lead to the transformation without inducing layer thinning [31] or damaging [32], we monitored the Raman spectrum in real time for different laser powers. We kept the exposure time the same (30 s) in order to avoid any time-dependent effects. Fig. 2(a) shows the Raman spectra of a 6-nm-thick flake at different powers, which are normalized to the incident laser power. At low power, the J_1–J_3 peaks at 155, 230, and 330 cm^{-1} can be clearly seen, while the E^1_{2g} and A_{1g} peaks have low intensity, indicating the presence of a small residual areas of the 2H phase. All peaks have a higher intensity than the ones in Fig. 1 due to the larger thickness of the flake in this case. From 0.3 mW and above, the intensity of the E^1_{2g} and A_{1g} peaks from the 2H phase increases, while the intensities of the peaks belonging to the 1T/1T′ polymorphs decrease. This change indicates that the gradual increase (decrease) of the 2H (1T/1T′) phase content within the flake.

The response of MoS_2 to different laser powers can be better understood by investigating the behavior of the integrated intensity ratio of the A_{1g} to the J_3 peak. We choose these two peaks for a more accurate fit at low fluence but the analogous behavior is observed for the ratio of the E^1_{2g} to the J_1 or J_3 peak. Fig. 2(b) shows a logarithmic plot of the intensity ratio of A_{1g} to the J_3 peak as a function of the laser power for two different flakes with a thickness of 6 and 23 nm. As can be seen, the behavior is similar in the two flakes and the ratio of the intensities does not change up to 0.4 mW. Between 0.4 and 1 mW, the response of the material changes as the intensity of the E^1_{2g} peak increases relative to that of J_3. At these powers, the percentage of the 2H phase is increasing exponentially. Above 1.5 mW, the ratio of the two intensities from the flake with a thickness of 23 nm slightly drops, which indicates degradation effects. It has been reported that the damage and etching occur for flakes with similar thicknesses above 1 mW [32]. Another feature of this plot is that the data follow an "exposure-response" relationship, meaning that the phase transition of the MoS_2 shows a sigmoidal dependence on the radiation power, similar to the growth behavior of several materials such as graphene [33], silver nanoparticles [34], and nanowires [35]. From a fit to the data by a Boltzmann sigmoidal function and the extrapolation of the linear part, we obtain the threshold power of about 0.5 mW, where the conversion of the 1T/1T′ to the 2H phase takes place for the 6-nm-thick sample. For the flake with a thickness of 23 nm, we find a threshold

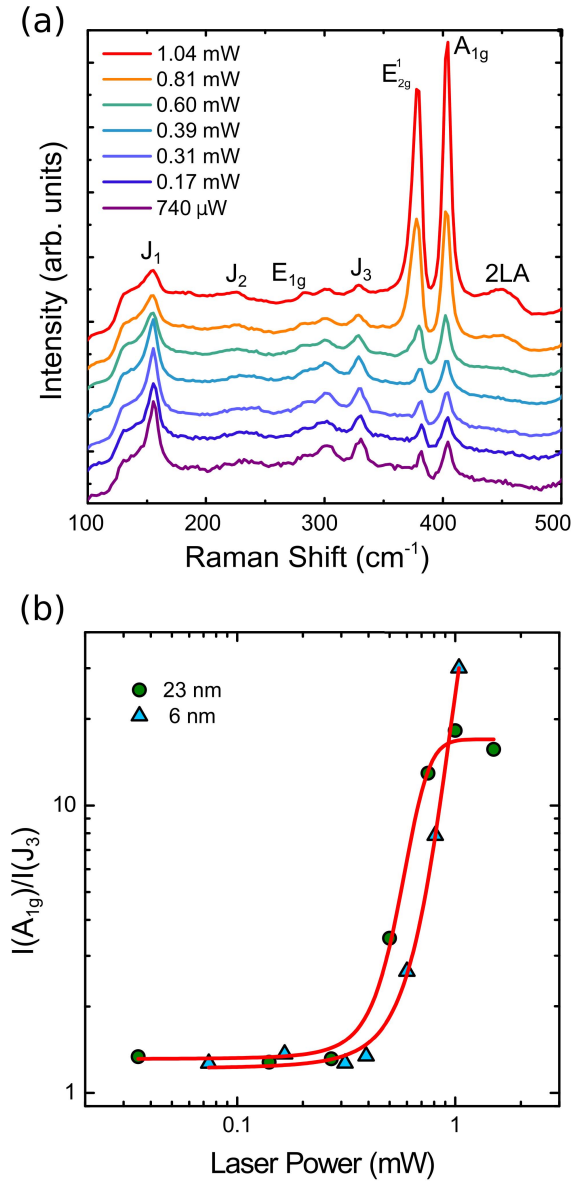

Fig. 2. Raman spectroscopy of laser-induced annealing on the 1T/1T′-MoS_2. (a) Evolution of the Raman spectrum of a 6-nm 1T/1T′-MoS_2 flake with increasing the laser power. As the laser power increases, the E^1_{2g} and A_{1g} peaks from the 2H phase of the MoS_2 become more prominent. (b) Relative intensity ratio of the A_{1g} to J_3 peak as a function of the laser power accompanied by Boltzmann sigmoidal function fit for two flakes with thickness 6 and 23 nm. The behavior of the two different in thickness flakes is similar.

of 0.4 mW. This slight lower value is expected as a higher fraction of the incoming photons is absorbed by the thicker MoS_2. It is worth mentioning that while the E^1_{2g} and A_{1g} Raman peaks are restored, this does not occur for the exciton peaks in the photoluminescence spectrum, suggesting non-radiative recombination processes between the electron-hole pairs. Possible mechanisms are electron-hole separation due to remaining 1T/1T′ phase patches [36] or relaxation of the exited electrons through gap states from defects. This observation is in good agreement with studies of the photoluminescence spectra from chemically exfoliated few-layer MoS_2 (∼10 nm) after annealing [37].

Moving a step further, by exploiting LP, we study the creation of lateral heterostructures of 1T/1T′- and 2H-MoS_2 [Fig. 3(a)]. The devices were fabricated from mechanically exfoliated MoS_2flakes, transferred onto SiO_2 (285 nm)/Si substrates using the dry transfer technique explained in [38], followed by the standard electron beam (*e*-beam) lithography and metal deposition of Ti/Au contacts. After the devices were immersed in BuLi for more than 24 h, the transformation takes place. The flakes were subsequently exposed to laser radiation and the resulting electrical characteristics were studied.

Most of the lithiated MoS_2 devices show a weak modulation of the conductance with the back-gate voltage [Fig. 3(c)]. This has been observed in other studies and it is due to the high concentration of the carriers in the channel [27], [37], [39]. Furthermore, in one case [see device D in Fig. 3(c)], we observed a relatively stronger and positive transconductance, possibly as a result of a higher content of the 2H phase remnants within the channel.

For the patterning of the semiconducting channel of the devices, we scribed a ∼0.5-μm-long line across the width of the devices with a laser power of ∼1 mW per spot that has a diameter of 500 μm. Fig. 3(b) shows an atomic force microscopy (AFM) image of the topography of the device with a laser-patterned channel. The laser-treated narrow channel between the source and drain is evident. In agreement with Guo *et al.* [20], we find that laser-treated areas have a lower thickness than the untreated ones (7 nm for the untreated and 5.8 nm for the laser-patterned part). This change in the thickness is around 20%–30%. Chemically exfoliated samples of 1T/1T′-MoS_2 are also thicker than the flakes of mechanically exfoliated MoS_2 [37]. A possible explanation is a difference in the structure of the two phases as suggested in [20]. Also, the possibility of intercalation of LiOH or other sources of contaminants between the layers from the chemical treatment should not be excluded.

After laser exposure, we investigated the electrical behavior of several devices and we did not observe a full restoration of the intrinsic semiconducting properties from the channel in most of the devices [Fig. 3(d)]. The transconductance in most of the channels became positive but with a negligible ON/OFF ratio [see devices A–C in Fig. 3(d)]. Furthermore, a tenfold decrease in the conductance compared to the BuLi-treated devices was observed that can be attributed to possible defect formation or oxidation from the exposure to the radiation.

In one case, a restoration of the semiconducting properties of the device was found. To compare the device characteristics before any treatment and after the final LP, we plotted the conductance of device D (with a thickness of three layers), as a function of the gate voltage, for the intrinsic channel, after the treatment with BuLi and after the LP of a thin semiconducting strip (see Fig. 4). As it can be seen, the conductance of the device has been reduced by more than an order of magnitude after the LP, in comparison to the intrinsic channel. Moreover, the field-effect mobility that was calculated based on the relation: $\mu = (L/W)(dG/dV_g)(1/C_{ox})$, with L being the length of the channel, W being the width of the channel, and $C_{ox} = 1.21 \times 10^{-4}$ Fm^{-2} being the gate capacitance per

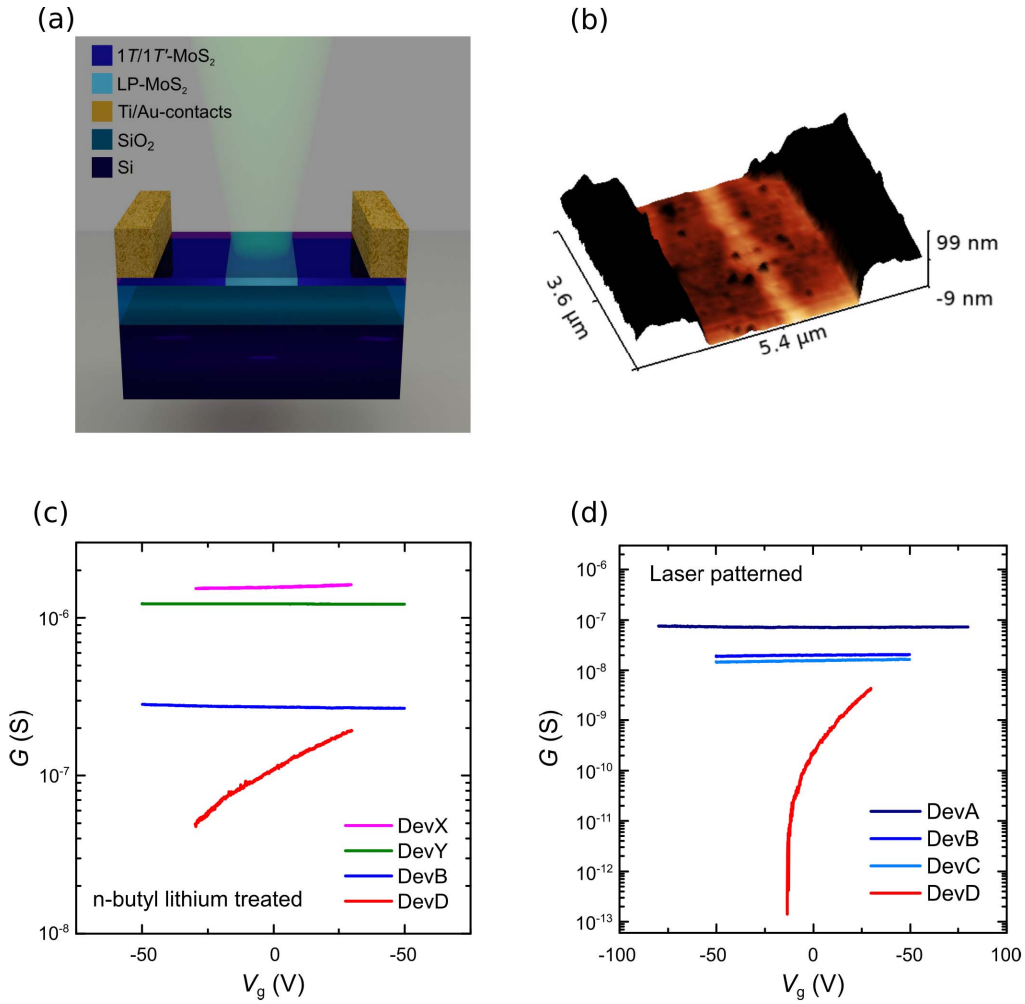

Fig. 3. Investigating the laser-induced phase transitions of a few-layer MoS_2 FET. (a) Illustration of a device, where the laser is patterning a strip of the flake to create the semiconducting 2H-MoS_2 channel. (b) 3-D AFM topographic image of a device (B) after LP of a narrow strip in the middle of the channel with a laser power of ∼1 mW and spot size of 500 nm. The strip in the middle of the channel has an approximate width of 400 nm and corresponds well with the laser treated portion of the MoS_2. (c) Conductance as a function of the back-gate voltage from four 1T/1T′-MoS_2 devices directly after the chemical treatment with BuLi. The poor modulation of the conductance from the back-gate voltage indicates the high-carrier-concentration in the devices. (d) Conductance as a function of the back-gate voltage from four devices after patterning a strip in the middle of the transistors as illustrated in (a) and shown in (b). In most devices, the modulation of the conductance from the back-gate voltage is still negligible, which illustrates the ineffective laser-induced phase change.

unit area, reduced from 3.2 $cm^2\ V^{-1}\ s^{-1}$ before the chemical treatment to 1.1 $cm^2\ V^{-1}\ s^{-1}$ after the LP. On the other hand, there was an improvement to the values of the subthreshold swing that decreased to 0.6 V/dec.

The fact that even after the LP, there is no restoration of the semiconducting behavior in most of our devices, while the Raman spectra show the reappearance and increase in the intensity of the E_{2g} and A_{1g} peaks, which are not surprising. Recent studies on the phase conversion of Li-treated MoS_2 through X-ray photoelectron spectroscopy (XPS) and Raman showed similar discrepancies between the two techniques [40]. While the Raman peaks of the 1T phase reduced and the peaks of the 2H phase increase upon laser annealing, the XPS data show that there is still a significant amount of 1T/1T′ phase content within the flakes. Also, FETs that were annealed at 123 °C still show a negligible resistance variation when the back gate is applied [40]. These discrepancies among the different characterization techniques attributed to the different cross sections of the Raman scattering between the different MoS_2 phases. Therefore, the reason for the very weak transconductance and low ON/OFF ratio in our laser-patterned devices is most likely due to a significant remaining content of 1T/1T′-MoS_2, which screens the electric field from the back gate and is undetectable with the Raman spectroscopy. This could also be the explanation of the nonrestored photoluminescence spectra as noted earlier. The difference between restored annealed devices from previous studies and the laser patterned ones here is that in the former case annealing takes place in an inert environment and for longer durations for a successful restoration [24], [37]. The laser-induced local annealing under normal conditions here seems to be insufficient to restore completely the 2H phase within 30 s and is most likely to promote defect formation and even oxidation [40], additionally, which result in lower conductance of laser patterned devices. The degradation of the devices during the exposure could be resolved if such laser scribing

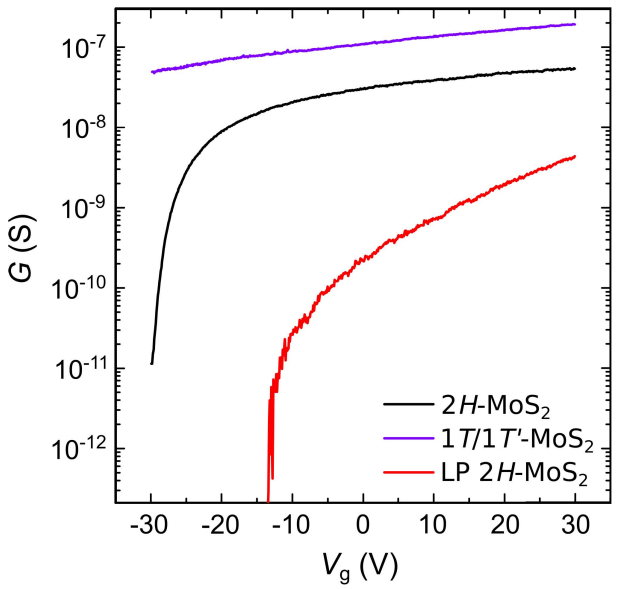

Fig. 4. Comparison of the different treatments to the characteristics of device D. Conductance as a function of the back-gate voltage for the intrinsic 2H-MoS_2 (black), after the treatment with BuLi (blue) and after the LP of a semiconducting channel (red).

process would be performed under vacuum or inert atmosphere conditions.

III. Conclusion

In summary, we have studied the metallic to semiconducting phase transition in thin MoS_2 flakes by radiation with a continuous wave green laser. We found that the laser power range, in which the intensity Raman peaks from the 2H phase start to increase, is in the range of 0.3–1 mW. Using controlled LP in several MoS_2 devices, we find that in most of the devices, the *n*-type semiconducting characteristic of MoS_2 is not restored, while the electrical properties degrade possibly due to defect formation or oxidation of the exposed area. This paper shows that the polymer-based patterning and chemical treatment [23] is the best route to obtain on demand for novel heterostructures from the various MoS_2 phases. Finally, our work suggests that any assessment of metallic to semiconducting transitions in TMDCs should be realized via photoluminescence or XPS characterization techniques.

Acknowledgment

The authors would like to thank D. Voiry for his suggestions regarding the chemical intercalation process, W. Ewers for his assistance at the glove box facilities, and A. Castellanos-Gomez for measurements at his facilities and for discussion.

References

[1] Q. H. Wang, K. Kalantar-Zadeh, A. Kis, J. N. Coleman, and M. S. Strano, "Electronics and optoelectronics of two-dimensional transition metal dichalcogenides," *Nature Nanotechnol.*, vol. 7, no. 11, pp. 699–712, Nov. 2012, doi: 10.1038/nnano.2012.193.

[2] M. Chhowalla, H. S. Shin, G. Eda, L.-J. Li, K. P. Loh, and H. Zhang, "The chemistry of two-dimensional layered transition metal dichalcogenide nanosheets," *Nature Chem.*, vol. 5, no. 4, pp. 263–275, 2013, doi: 10.1038/nchem.1589.

[3] H. Li, J. Wu, Z. Yin, and H. Zhang, "Preparation and applications of mechanically exfoliated single-layer and multilayer MoS_2 and WSe_2 nanosheets," *Accounts Chem. Res.*, vol. 47, no. 4, pp. 1067–1075, 2014, doi: 10.1039/C5CS00106D.

[4] M. Buscema *et al.*, "Photocurrent generation with two-dimensional van der Waals semiconductors," *Chem. Soc. Rev.*, vol. 44, no. 11, pp. 3691–3718, 2015, doi: 10.1039/C5CS00106D.

[5] K. F. Mak, C. Lee, J. Hone, J. Shan, and T. F. Heinz, "Atomically thin MoS_2: A new direct-gap semiconductor," *Phys. Rev. Lett.*, vol. 105, no. 13, p. 136805, 2010, doi: 10.1103/PhysRevLett.105.136805.

[6] H. Bergmann, B. Czeska, I. Haas, B. Mohsin, and K.-H. Wandner, *Gmelin Handbook of Inorganic and Organometallic Chemistry*, vol. B7. Berlin, Germany: Springer-Verlag, 1992.

[7] B. Radisavljevic, A. Radenovic, J. Brivio, V. Giacometti, and A. Kis, "Single-layer MoS_2 transistors," *Nature Nanotechnol.*, vol. 6, pp. 147–150, Jan. 2011, doi: 10.1038/nnano.2010.279.

[8] O. Lopez-Sanchez, D. Lembke, M. Kayci, A. Radenovic, and A. Kis, "Ultrasensitive photodetectors based on monolayer MoS_2," *Nature Nanotechnol.*, vol. 8, pp. 497–501, Jun. 2013, doi: 10.1038/nnano.2013.100.

[9] F. Withers *et al.*, "Light-emitting diodes by band-structure engineering in van der Waals heterostructures," *Nature Mater.*, vol. 14, pp. 301–306, Feb. 2015, doi: 10.1038/nmat4205.

[10] K. Chrissafis *et al.*, "Structural studies of MoS_2 intercalated by lithium," *Mater. Sci. Eng., B*, vol. 3, nos. 1–2, pp. 145–151, 1989, doi: 10.1016/0921-5107(89)90194-3.

[11] F. Wypych and R. Schöllhorn, "1T-MoS_2, a new metallic modification of molybdenum disulfide," *J. Chem. Soc., Chem. Commun.*, no. 19, pp. 1386–1388, 1992. [Online]. Available: https://pubs.rsc.org/en/journals/journalissues/c3#!issueid=c31995_0_24&type=archive&issnprint=0022-4936, doi: 10.1039/C39920001386.

[12] E. Benavente, M. A. Santa Ana, F. Mendizábal, and G. González, "Intercalation chemistry of molybdenum disulfide," *Coordination Chem. Rev.*, vol. 224, nos. 1–2, pp. 87–109, 2002, doi: 10.1016/S0010-8545(01)00392-7.

[13] M. B. Dines, "Lithium intercalation via n-Butyllithium of the layered transition metal dichalcogenides," *Mater. Res. Bull.*, vol. 10, no. 4, pp. 287–291, 1975, doi: 10.1016/0025-5408(75)90115-4.

[14] N. Imanishi, M. Toyoda, Y. Takeda, and O. Yamamoto, "Study on lithium intercalation into MoS_2," *Solid State Ionics*, vol. 58, nos. 3–4, pp. 333–338, 1992, doi: 10.1016/0167-2738(92)90137-E.

[15] F. Xiong *et al.*, "Li intercalation in MoS_2: *In situ* observation of its dynamics and tuning optical and electrical properties," *Nano Lett.*, vol. 15, no. 10, pp. 6777–6784, 2015, doi: 10.1021/acs.nanolett.5b02619.

[16] D. Voiry, A. Mohite, and M. Chhowalla, "Phase engineering of transition metal dichalcogenides," *Chem. Soc. Rev.*, vol. 44, no. 9, pp. 2702–2712, 2015, doi: 10.1039/C5CS00151J.

[17] M. Azhagurajan, T. Kajita, T. Itoh, Y.-G. Kim, and K. Itaya, "*In situ* visualization of lithium ion intercalation into MoS_2 single crystals using differential optical microscopy with atomic layer resolution," *J. Amer. Chem. Soc.*, vol. 138, no. 10, pp. 3355–3361, 2016, doi: 10.1021/jacs.5b11849.

[18] S. J. Sandoval, D. Yang, R. F. Frindt, and J. C. Irwin, "Raman study and lattice dynamics of single molecular layers of MoS_2," *Phys. Rev. B, Condens. Matter*, vol. 44, no. 8, p. 3955, 1991, doi: 10.1103/PhysRevB.44.3955.

[19] X. Fan *et al.*, "Fast and efficient preparation of exfoliated 2H MoS_2 nanosheets by sonication-assisted lithium intercalation and infrared laser-induced 1T to 2H phase reversion," *Nano Lett.*, vol. 15, no. 9, pp. 5956–5960, 2015, doi: 10.1021/acs.nanolett.5b02091.

[20] Y. Guo *et al.*, "Probing the dynamics of the metallic-to-semiconducting structural phase transformation in MoS_2 crystals," *Nano Lett.*, vol. 15, no. 8, pp. 5081–5088, 2015, doi: 10.1021/acs.nanolett.5b01196.

[21] G. Eda, T. Fujita, H. Yamaguchi, D. Voiry, M. Chen, and M. Chhowalla, "Coherent atomic and electronic heterostructures of single-layer MoS_2," *ACS Nano*, vol. 6, no. 8, pp. 7311–7317, 2012, doi: 10.1021/nn302422x.

[22] R. Kappera *et al.*, "Metallic 1T phase source/drain electrodes for field effect transistors from chemical vapor deposited MoS_2," *APL Mater.*, vol. 2, no. 9, p. 092516, 2014, doi: 10.1063/1.4896077.

[23] R. Kappera *et al.*, "Phase-engineered low-resistance contacts for ultrathin MoS_2 transistors," *Nature Mater.*, vol. 13, pp. 1128–1134, Aug. 2014, doi: 10.1038/nmat4080.

[24] Y. Ma *et al.*, "Reversible semiconducting-to-metallic phase transition in chemical vapor deposition grown monolayer WSe_2 and applications for devices," *ACS Nano*, vol. 9, no. 7, pp. 7383–7391, 2015, doi: 10.1021/acsnano.5b02399.

[25] A. Allain, J. Kang, K. Banerjee, and A. Kis, "Electrical contacts to two-dimensional semiconductors," *Nature Mater.*, vol. 14, no. 12, pp. 1195–1205, 2015, doi: 10.1038/nmat4452.

[26] D. Voiry *et al.*, "Conducting MoS_2 nanosheets as catalysts for hydrogen evolution reaction," *Nano Lett.*, vol. 13, no. 12, pp. 6222–6227, 2013, doi: 10.1021/jacs.6b13238.

[27] N. Papadopoulos, G. A. Steele, and H. S. J. van der Zant, "Efros-Shklovskii variable range hopping and nonlinear transport in $1T/1T'$-MoS_2," *Phys. Rev. B, Condens. Matter*, vol. 96, no. 23, p. 235436, 2017, doi: 10.1103/PhysRevB.96.235436.

[28] X. Chen, Z. Chen, and J. Li, "Critical electronic structures controlling phase transitions induced by lithium ion intercalation in molybdenum disulphide," *Chin. Sci. Bull.*, vol. 58, no. 14, pp. 1632–1641, 2013, doi: 10.1007/s11434-013-5834-y.

[29] X. Rocquefelte, F. Boucher, P. Gressier, G. Ouvrard, P. Blaha, and K. Schwarz, "Mo cluster formation in the intercalation compound $LiMoS_2$," *Phys. Rev. B*, vol. 62, no. 4, pp. 2397–2400, 2000, doi: 10.1103/PhysRevB.62.2397.

[30] A. P. Nayak *et al.*, "Pressure-dependent optical and vibrational properties of monolayer molybdenum disulfide," *Nano Lett.*, vol. 15, no. 1, pp. 346–353, 2015, doi: 10.1021/nl5036397.

[31] A. Castellanos-Gomez, M. Barkelid, A. M. Goossens, V. E. Calado, H. S. J. van der Zant, and G. A. Steele, "Laser-thinning of MoS_2: On demand generation of a single-layer semiconductor," *Nano Lett.*, vol. 12, no. 6, pp. 3187–3192, 2012, doi: 10.1021/nl301164v.

[32] S. Sahoo, A. P. S. Gaur, M. Ahmadi, M. J.-F. Guinel, and R. S. Katiyar, "Temperature-dependent raman studies and thermal conductivity of few-layer MoS_2," *J. Phys. Chem. C*, vol. 117, no. 17, pp. 9042–9047, 2013, doi: 10.1021/jp402509w.

[33] N. S. Mueller, A. J. Morfa, D. Abou-Ras, V. Oddone, T. Ciuk, and M. Giersig, "Growing graphene on polycrystalline copper foils by ultra-high vacuum chemical vapor deposition," *Carbon*, vol. 78, pp. 347–355, Nov. 2014, doi: 10.1016/j.carbon.2014.07.011.

[34] N. T. K. Thanh, N. Maclean, and S. Mahiddine, "Mechanisms of nucleation and growth of nanoparticles in solution," *Chem. Rev.*, vol. 114, no. 15, pp. 7610–7630, 2014, doi: 10.1021/cr400544s.

[35] S. Fernández-Garrido, J. K. Zettler, L. Geelhaar, and O. Brandt, "Monitoring the formation of nanowires by line-of-sight quadrupole mass spectrometry: A comprehensive description of the temporal evolution of GaN nanowire ensembles," *Nano Lett.*, vol. 15, no. 3, pp. 1930–1937, 2015, doi: 10.1021/nl504778s.

[36] J. Zhu *et al.*, "Argon plasma induced phase transition in monolayer MoS_2," *J. Amer. Chem. Soc.*, vol. 139, no. 30, pp. 10216–10219, 2017, doi: 10.1021/jacs.7b05765.

[37] G. Eda, H. Yamaguchi, D. Voiry, T. Fujita, M. Chen, and M. Chhowalla, "Photoluminescence from chemically exfoliated MoS_2," *Nano Lett.*, vol. 11, no. 12, pp. 5111–5116, 2011, doi: 10.1021/nl201874w.

[38] A. Castellanos-Gomez *et al.*, "Deterministic transfer of two-dimensional materials by all-dry viscoelastic stamping," *2D Mater.*, vol. 1, no. 1, p. 011002, 2014, doi: 10.1088/2053-1583/1/1/011002.

[39] J. S. Kim *et al.*, "Electrical transport properties of polymorphic MoS_2," *ACS Nano*, vol. 10, no. 8, pp. 7500–7506, 2016, doi: 10.1021/acsnano.6b02267.

[40] J. Kim *et al.*, "Phase conversion of chemically exfoliated molybdenum disulfide," *Current Appl. Phys.*, vol. 17, no. 1, pp. 60–65, 2017, doi: 10.1016/j.cap.2016.11.001.

Authors' photographs and biographies not available at the time of publication.